DESIGN AND OPTIMIZATION OF COMPOSITE LAYERING FOR A MEDIUM-SIZED UAV WING

Le Thi Tuyet Nhung[1,*], Vu Dinh Quy[1], Pham Quang Minh[1], Nguyen Le Minh[2], Tran Dinh Thang[2]

DOI: http://doi.org/ 10.57001/huih5804.2025.256

ABSTRACT

This study focuses on the design and optimization of a composite wing for a medium-range UAV inspired by the Heron model, aiming to minimize structural weight while meeting safety and performance criteria. When comparing the stress and displacement results of spars with different geometric cross-sections under identical conditions, the rectangular spar performed the best and was thus chosen for the wing configuration to proceed with optimization steps. The 16.6m span wing comprises components such as skin, spars, and ribs, using materials including several types of composites, foam, and epoxy resin. The design was analyzed under static distributed loads applied on two wing spars, with load factors ranging from 3.86g to -1.5g. Using Schrenk's lift distribution and finite element analysis (FEA) with the Tsai-Wu failure criterion, optimization iterations reduced weight by 20% - from 176kg to 142kg - while maintaining a minimum safety of 1.5 and limiting maximum deformation to 723mm. Among the tested fiber orientations, simulation results show that a 0° orientation is the most optimal. Results demonstrate the potential of advanced material and structural optimization in achieving lightweight, high-performance UAV wings.

Keywords: *Wing structure, composite, Finite Element Method.*

[1]Hanoi University of Science and Technology, Vietnam
[2]Viettel High Technology Industries Corporation, Vietnam
[*]Email: nhung.lethituyet@hust.edu.vn

Received: 01/3/2025
Revised: 10/5/2025
Accepted: 25/7/2025

1. INTRODUCTION

Nowadays, UAVs are widely used, especially in the military sector. One of the most important components of both UAVs and aircraft is the wing. Optimizing the wing is essential to enhance efficiency in both technical and economic aspects. Some studies focus on the external structure of the wing to improve performance, such as those by Bino [1] and Basri [2]. Additionally, to reduce wing weight, Manjari [3] and Rai [4] have compared different wing materials. Meanwhile, Sullivan and Rajadurai have pursued wing optimization through fiber orientation.

This study aims to design and optimize a Heron UAV wing under static loading with Schrenk Lift Distribution. Initial calculations will be validated using Ansys to select the best spar cross-section among rectangular, I-beam, and C-beam designs under identical conditions. A composite wing model will then be developed using zone-based material distribution inspired by Rajpal [5]. In the first optimization phase, weight reduction will follow Shangru [6] and Sekar's [7] approaches, focusing on spar layer reduction as per Hutagalung [8]. The optimization will ensure compliance with Tsai-Wu safety criteria and FAR23 displacement standards. Finally, the impact of composite fiber orientation on static load performance will be analyzed to identify the optimal fiber configuration.

2. MODEL

2.1. Wing spar geometry

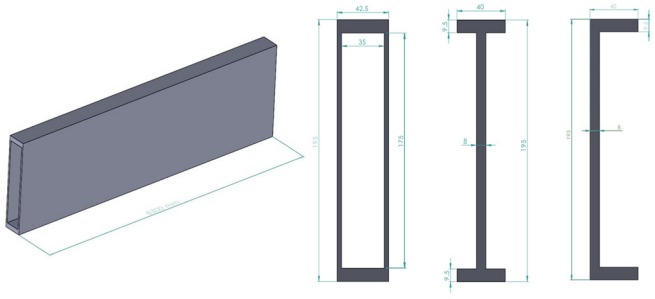

Fig. 1. Spar cross sections

During the survey, we found that the majority of UAV wings currently use three types of beams: rectangular beams, I-beams, and C-beams. Thus, these types of beams are considered to determine the optimal cross-sectional shape to be incorporated into the overall wing model. For simplicity, the beams are assumed to be made

of an isotropic material with a modulus of elasticity $E = 1.23 \times 10^{11}$Pa, a length of 8.3m, and fixed at one end. Note that the cross-sectional areas of the three beam types are all equal to 2163mm^2 to ensure their masses are the same. Also, their heights are identical (195mm) to fit the wing model. The cross-sectional drawings of the three beam types are provided in Fig. 1.

2.2. Completed wing model & Materials

The geometric model of the wing was created using SolidWorks software, referencing the UAV Heron wing design (see Fig. 2). The model includes the main components: wing skin (upper and lower skins), main spar, rear spar and 30 ribs distributed along the span.

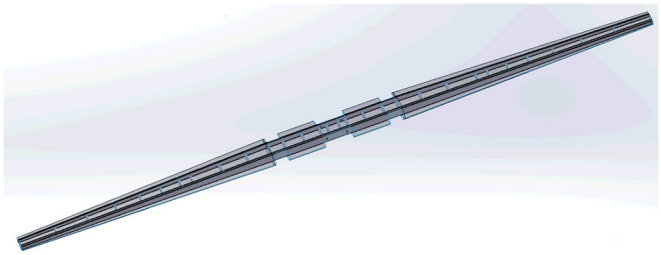

Fig. 2. Wing model overview

In this model, each part will use a combination of different composite materials. The thickness of each layer of composite C, UD, S is 0.26mm, 0.53mm and 0.09mm, respectively. Material properties are listed in Table 1.

Table 1. Material properties

	C	UD	Foam	S	Epoxy
Density (kg/m^3)	1484	1518	75	1993	1160
E_1 (Pa)	5.03e10	1.23e11	9.2e7	3.71e10	3.78e9
E_2 (Pa)	5.03e10	7.78e9		3.71e10	
E_3 (Pa)	7.06e9	7.78e9		1.88e10	
v_{12}	3.31e-2	0.27	0.25	0.13	0.35
v_{13}	3.87e-1	0.27		0.33	
v_{23}	3.87e-1	0.42		0.33	
G_{12} (Pa)	2.65e9	5.00e9	3.68e7	6.21e9	1.40e9
G_{13} (Pa)	2.43e9	5.00e9		5.05e9	
G_{23} (Pa)	2.43e9	3.08e9		5.05e9	

2.3. Configuration

The initial configuration (Version 1) is given as follows:

The Wing Skin are divided into three sections: Zone 1 in the center, and Zone 2 on the left and right sides of the wing. Note that Zone 1B and Zone 2B are the connection areas between Wing Skin and Spars Cap (see Fig. 3). The configuration in each zone is shown in Table 2.

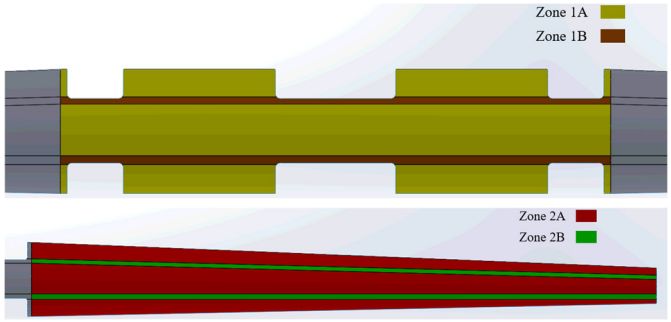

Fig. 3. Zone 1 and zone 2 in Wing Skin

Main Spar and Rear Spar are divided into three components: spar cap, spar web, and spar core. The Spars core is made of foam, while the main spar web and rear spar web consists of 15 and 10 layers of Carbon fabric (C) on each side, respectively. The Spar cap is divided into three zones along the spar's length (see Fig. 4). The rear spar has a configuration of 40 layers of UD in Zone 1, 30 layers of UD in Zone 2, and 20 layers of UD in Zone 3. The rear spar has a configuration of 20 layers of UD in Zone 1, 15 layers of UD in Zone 2, and 10 layers of UD in Zone 3. All the ribs have the same structure: 2C/Foam 10mm/2C.

Table 2. Configuration in each Wing Skin zone

Zone	Ply Pattern
1A	2C/Foam 10 mm/2C/S
1B	2C/15UD/2C/S
2A	C/Foam 10 mm/2C/S
2B	2C/5UD/2C/S

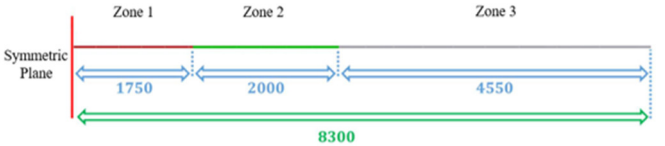

Fig. 4. Spar Cap Configuration

3. METHODOLOGY

3.1. Load factor

In aeronautics, the load factor (n = L/W) is the ratio of the lift of an aircraft to its weight and represents a global measure of the stress to which the structure of the aircraft is subjected. For the UAV wing under consideration, the load factor ranges from 3.86g to -1.5g according to FAR 23. In the case 3.86g and -1.5g, the lift force acting on the wing are 39689N and -13612N, respectively.

3.2. Schrenk Lift Distribution

Schrenk's method is an approach to estimate the lift distribution along the span of a wing. Schrenk's method assumes that the actual lift distribution on a wing is somewhere between a uniform distribution and an

elliptical distribution. The actual lift distribution is then approximated by taking the average of these two distributions.

$$L'_{Elliptical} = \frac{4L}{\Pi b}\sqrt{1-\left(\frac{2y}{b}\right)^2} \quad (1)$$

$$L'_{Planform} = \frac{2L}{(1+\lambda)b}\left(1+\frac{2y}{b}(\lambda-1)\right) \quad (2)$$

$$L'_{Schrenk} = \frac{L'_{Elliptical} + L'_{Planform}}{2} \quad (3)$$

Where L is total lift force (N), L' is lift distribution (N/m), λ is taper ratio, b is wingspan (m), y is spanwise distance of section (m).

On the aircraft wing, spars are the primary load-bearing components. Assuming the load on the wing is entirely distributed between the two spars, with 80% on the main spar and 20% on the rear spar, Schrenk's method is applied. Both the main and rear spars are divided into 20 equal segments per wing side. For the load factor of 3.86g, the load distribution graph is shown in Fig. 5, where segment 1 to segment 20 corresponds to wing root to wing tip:

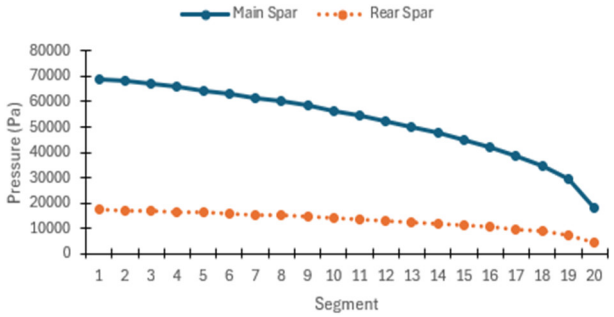

Fig. 5. Load values applied to beam span

3.3. Tsai-Wu failure criteria

The Tsai–Wu failure criterion is a phenomenological material failure theory widely used for anisotropic composite materials with different tensile and compressive strengths. The Tsai–Wu criterion predicts failure when the damage index in the laminate reaches 1. This failure criterion can be expressed as:

$$F_j\sigma_j + F_{ij}\sigma_i\sigma_j \leq 1 \text{ for } i, j = 1, 2, \ldots 6 \quad (4)$$

4. RESULT

4.1. Spar cross-section selection

Considering the case of the maximum load factor of 3.86g, the wing's lift force is 39689N. The main spar carries 80% of the load as previously mentioned, resulting in a load of 31751N on the main spar. For a spar length of 8.3m, corresponding to half the wingspan, the force applied to the spar is 15875.5N. The distributed load per unit length, q = 1912.7 (N/m). The stress and deformation of rectangular beam are shown in Fig. 6 and Fig. 7.

Fig. 6. Stress result of rectangular beam

Fig. 7. Deformation result of rectangular beam

Table 3 shows the comparison between beam theory and Ansys. Theoretical analysis shows that the rectangular cross-section has the smallest stress and displacement, making it the most efficient load-bearing cross-section for the beam. The comparison results between simulation and theory show minimal deviation, demonstrating that the accuracy of this simulation method is reliable.

Table 6. Comparison between Beam Theory and Ansys Result

	Beam Theory		Ansys Result	
	Max Stress (MPa)	Max Deformation (mm)	Max Stress (MPa)	Max Deformation (mm)
Rectangular	604.3	867	598.5	868
I-shaped	631.0	906	677.6	906
C-shaped	631.0	906	703.8	936

4.2. Results of version 1

The version 1 model is imported to ANSYS workbench for meshing and solving. In this model, there are 194225 nodes with 109344 elements. On the main spar and rear spar, there are a total of four holes, which serve as attachment points for bolts connecting the wing to the fuselage. Therefore, in this numerical analysis model, these four holes are fully constrained in all degrees of freedom (see Fig. 8). The force acting on the wing is represented as pressure, with 80 load application points corresponding to the distribution described above (see Fig. 9).

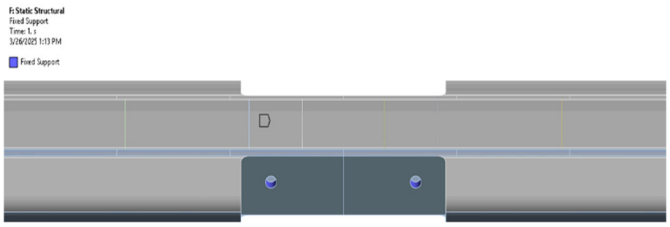

Fig. 8. Model constraint

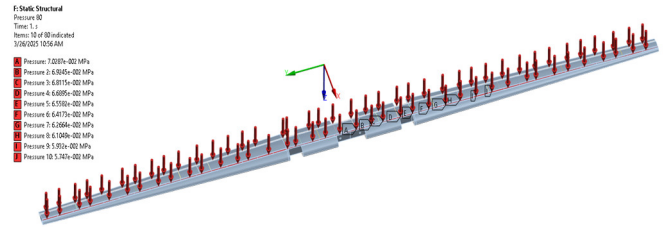

Fig. 9. Applied force

After the setup process, the wing's deformation, stress distribution, and the factor of safety (FOS) for each component are analyzed. The results are presented in Figs. 10 - 15.

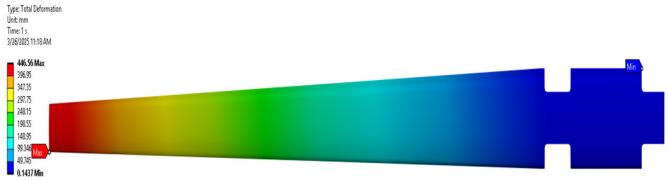

Fig. 10. Wing deformation

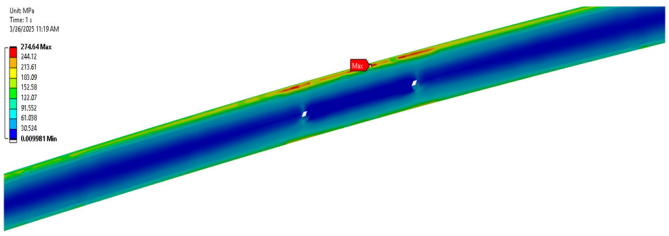

Fig. 11. Main spar stress

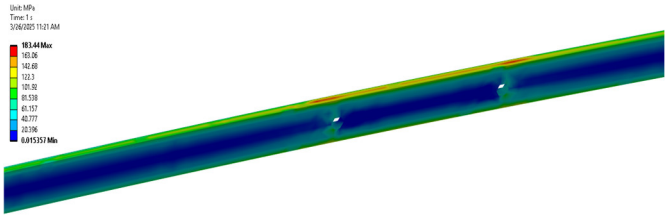

Fig. 12. Rear spar stress

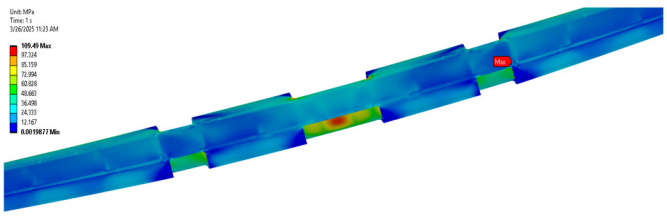

Fig. 13. Skin stress

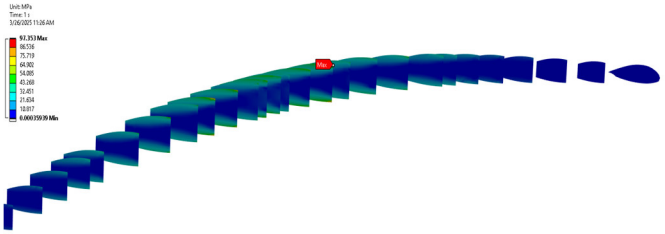

Fig. 14. Ribs stress

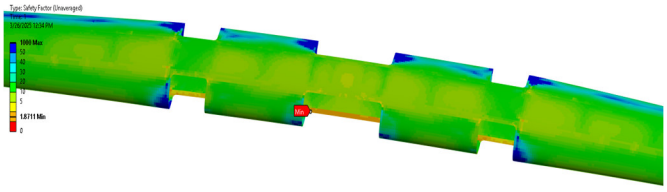

Fig. 15. Wing FOS

4.3. Correlation between ply configuration, deformation and FOS

To reduce the weight of the wing, the focus will be placed on decreasing the weight of the wing spars. The wing spars are constructed from multiple material layers, which differ across various zones. As a result, the number of material layers in each zone will be individually considered to analyze the relationship between the number of plies, deformation, and the FOS.

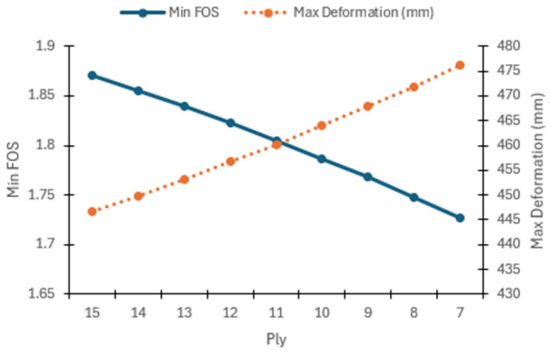

Fig. 16. Varying the number of plies in the main spar web

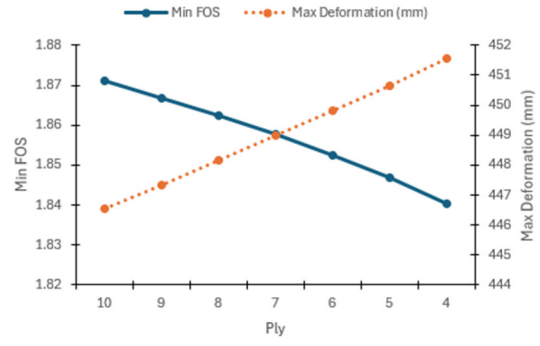

Fig. 17. Varying the number of plies in the rear spar web

Fig. 16 and Fig. 17 show the impact of the number of plies in the main spar web and rear spar web on FOS and

deformation. Overall, both graphs exhibit the same trend: as the number of plies increases, FOS decreases, and deformation increases. This is because reducing the number of material layers decreases the overall stiffness of the structure. However, Fig. 16 has a steeper slope compared to Fig. 17, meaning that changes in the number of layers in the main spar have a greater effect on the results than in the rear spar.

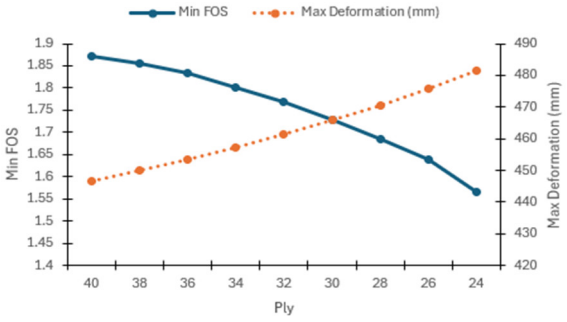

Fig. 18. Varying the number of ply in the main spar cap (Zone 1)

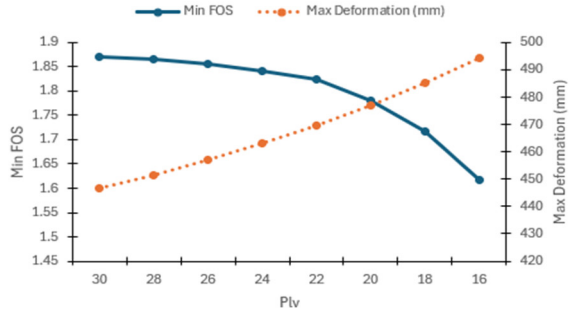

Fig. 19. Varying the number of ply in the main spar cap (Zone 2)

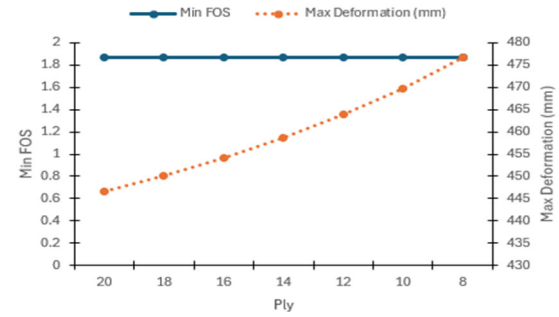

Fig. 20. Varying the number of ply in the main spar cap (Zone 3)

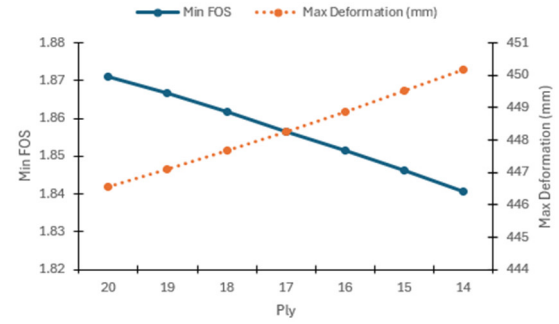

Fig. 21. Varying the number of ply in the rear spar cap (Zone 1)

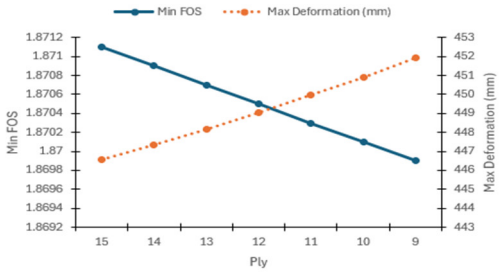

Fig. 22. Varying the number of ply in the rear spar cap (Zone 2)

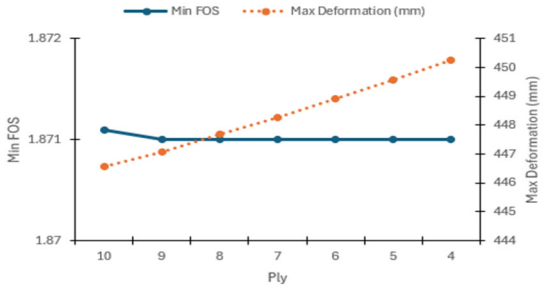

Fig. 23. Varying the number of ply in the rear spar cap (Zone 3)

Next, we consider the impact of the number of ply in the main spar caps and rear spar caps. Overall, the graphs show a clear trend: as the number of plies decreases, FOS decreases, while maximum deformation increases. This trend is most evident in Zone 1 and Zone 2 of both the main and rear spar caps, as these zones bear the highest loads. In contrast, Zone 3 shows minimal variation, since it experiences the least structural stress. For the main spar cap, Zone 1 (Fig. 18) and Zone 2 (Fig. 19) exhibit a significant drop in FOS and an increase in deformation as the number of plies decreases. Zone 3 (Fig. 20) remains relatively stable, with only minor changes in deformation. Similarly, in the rear spar cap, Zone 1 (Fig. 21) and Zone 2 (Fig. 22) follow the same trend of decreasing FOS and increasing deformation, while Zone 3 (Fig. 23) remains almost unchanged.

The most significant changes occur in Zone 1 of both spar caps, as this region endures the highest structural loads. Meanwhile, Zone 3 is the least sensitive to ply variation, indicating an opportunity for material optimization keeping more plies in Zone 1 and Zone 2 for structural integrity while reducing plies in Zone 3 to save material. This trend aligns with mechanical principles: fewer plies result in lower stiffness, reducing load-bearing capacity and increasing deformation.

4.4. Ply orientation

One of the factors affecting the safety factor and the strength of the spar is the fiber orientation in the layers. Fig. 24 shows the impact of fiber orientation on wing deformation and FOS. Min FOS is highest at 0° but

decreases sharply around 20 - 30°, then stabilizes at a lower level beyond 50°. Max Deformation is lowest at 0°, increases significantly around 30 - 40°, and remains high beyond this range.

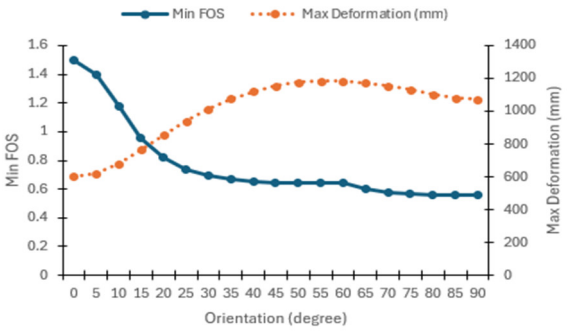

Fig. 24. Varying the ply orientation in the spars

4.5. Optimization version

From there, the optimal configuration is determined as follows:

Main spar cap in Zone 1, Zone 2, and Zone 3: 26 UD, 17 UD, and 10 UD, respectively, *Main spar web:* 8 C

Rear spar cap in Zone 1, Zone 2, and Zone 3: 15 UD, 10 UD, and 5 UD, respectively *Rear spar web:* 5 C

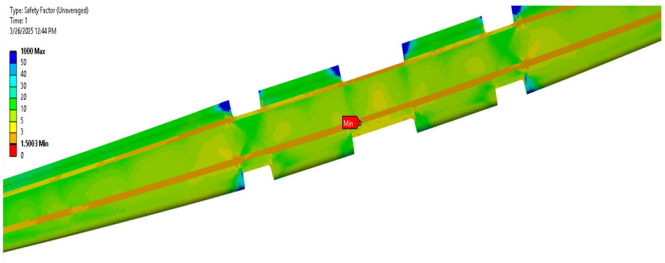

Fig. 25. FOS of new configuration wing

The simulation results show that the optimized wing meets the safety standard (≥ 1.5), satisfies the displacement requirement (≤ 723mm), reduces the wing mass from 176kg to 142kg.

5. CONCLUSION

Through comparative analysis of different spar cross-sections, the rectangular spar was determined to be the most effective in terms of stress distribution and deformation resistance. Finite element analysis (FEA) confirmed that an optimized fiber orientation of 0° provided the best balance between strength and minimal deformation. By refining the material configuration of the wing spars, the total wing mass was reduced from 176kg to 142kg an impressive 20% reduction while still ensuring a factor of safety above 1.5 and meeting the displacement limit of 723mm. These results demonstrate the potential of advanced composite materials and structural optimization techniques in enhancing UAV performance. By reducing the wing's weight by 20%, it is evident that the costs for materials and manufacturing will decrease. However, the exact manufacturing costs are confidential due to our commitment with our cooperation.

This work aims to give a procedure of preliminary structural design of a medium-size UAV. Future work can extend this research by considering additional load factors such as bending and torsion, dynamic flight conditions, and further material innovations. Incorporating real-world testing and wind tunnel experiments could further validate the findings and refine the wing's structural efficiency.

ACKNOWLEDGMENT

This study is funded by Hanoi University of Science and Technology (HUST) under grant number B2025-BKA-12. The authors are also grateful for the cooperation between Viettel Aerospace Institute and Hanoi University of Science for the support during this research.

REFERENCES

[1]. Bino Prince Raja, Ramanan G, "Static structural analysis and testing of aircraft wing spar using," *Materials Today: Proceedings,* 2022.

[2]. Ernie Illyani Basri, Faizal Mustapha, Mohamed Thariq, "Conceptual design and simulation validation based finite element optimisation for tubercle leading edge composite wing of an unmanned aerial vehicle," *Journal of Materials Research and Technology,* 2019.

[3]. A. Navya Manjari, R. Ajith Raj, N. Rajasekhar Rayudu, "Numerical and analytical analysis of wing spar made with different composite material," *Materials Today: Proceedings,* 2023.

[4]. Anuj Shankar Rai, Ashish Gupta, Manu Kumar, "Design and Analysis of General Aviation Aircraft Wings Using Different Materials," *International Journal of Innovative Research in Technology,* 9, 12, 2023.

[5]. D. Rajpal, F.M.A. Mitrotta, C.A. Socci, "Design and testing of aeroelastically tailored composite wing under fatigueand gust loading including effect of fatigue on aeroelastic performance," *Composite Structures,* 2021.

[6]. Shangru Xu, Yaolong Liu, Jifa Zhang, Yao Zheng, "Preliminary Design and Optimization of Primary Structures for a," *Aerospace,* 2024.

[7]. K Raja Sekar, M Ramesh, R Naveen, "Aerodynamic design and structural optimization of a wing for an Unmanned Aerial Vehicle (UAV)," in *IOP Conference Series: Materials Science and Engineering*, 2020.

[8]. M. R. A. Hutagalung, A. A. Latif, H. A. Israr, "Structural Design of UAV Semi-monoque Composite Wing," *Journal of Transport System Engineering,* 2016.